Floating wind farm design using social and environmental constraints

Journal of Physics: Conference Series **2767** (2024) 092081 doi:10.1088/1742-6596/2767/9/092081

Floating wind farm design using social and environmental constraints

Kutay Yilmazlar[1], Craig White[2], Stefano Cacciola[1], José Cândido[2], Alessandro Croce[1]

[1]Department of Aerospace Science and Technology, Politecnico di Milano, Milan, Italy.
[2]WavEC Offshore Renewables, Lisbon, Portugal.

E-mail: kutay.yilmazlar@polimi.it

Abstract. This work proposes a wind farm design methodology, integrating several design variables from different design aspects into an optimization problem, such as turbine power, number of turbines, cable types, wind farm layout and site location. A mixed integer genetic algorithm is employed to combine discrete and continuous design variables to find the design with minimum Levelized Cost of Energy (LCoE). The wind farm LCoE is calculated using a wind farm model, which combines detailed cost functions for different cost elements and engineering wake models to estimate Annual Energy Production. The design is constrained not only by technical aspects such as total power, farm area, but also by environmental and social constraints. These include the wind farm visibility, which is a popular concern among the people living along the coast of nearby wind farms, and availability, implying the compliance with the designated exclusion zones. To demonstrate the sensitivity of design constraints, two floating wind farms are sited and optimized as a case study, using different visibility constraints. The developed design tool within this study aims to bridge the gap between wind farm developers and local authorities who are responsible for permitting and zoning of development areas.

1. Introduction

As wind farms are increasingly deployed in offshore sites, the importance of design optimization becomes even more evident. In fact, onshore wind farm geometries mostly depend on terrain orography, whereas offshore environment offers a more flexible room for layout optimization. There has been a lot of effort studying the wind farm design in the literature, whose research focus span from initial feasibility analysis of a certain site to detailed wind farm design optimizations using different methods, for example, multiple criteria decision analysis [1] and multidisciplinary analysis and optimization [2].

Since the economics of the wind farms are usually evaluated by levelized cost of energy (LCOE), accurate assessment of project costs and energy generation is essential to deliver accurate LCOE values. This work employs such a wind farm cost model capable of modelling onshore, fixed-bottom and floating offshore wind farms and includes dynamic cost functions to accurately evaluate a project's financials at any time, instead of fixed static costs. In addition to the ever-growing wind turbine sizes, designers will face more challenges as farms are deployed in areas where only floating wind turbines are viable. Different from their fixed-bottom counterparts, floating wind farms include unique aspects that require special attention during the initial planning stage, as addressed by the recent work of Hietanen et al. [3]. Beside

optimizing the wind farm design to achieve the best economic metrics, new offshore wind farm installations are required to limit their environmental impact and to increase social acceptance, which could be tackled already during the design phase.

This work proposes a wind farm design methodology, integrating several design variables from different design aspects into an optimization problem. Hereby, in addition to the usual technical constraints, this study investigates the potential impact of social and environmental constraints on optimal wind farm designs. The focus is put on the wind farm visibility and compliance with the exclusion zones representing natural preserve areas. To demonstrate the sensitivity of these design constraints, a floating wind farm on the Atlantic coast of Iberian Peninsula is sited and optimized as a case study. In the following chapters, the wind farm design methodology and results from this case study are presented.

2. Methodology

2.1. Wind farm design optimization problem

An optimization problem based on minimizing wind farm LCOE is set up by incorporating several design parameters, denoted as $\boldsymbol{x}$ and $\boldsymbol{y}$ in the following, and constraints dealing with different aspects of wind farm development. The design optimization problem can be written in a general form:

$$\begin{aligned} \underset{\boldsymbol{x},\boldsymbol{y}}{\text{minimize}} \quad & LCOE(\boldsymbol{x},\boldsymbol{y}) \\ \text{subject to} \quad & \boldsymbol{x_{min}} \leq \boldsymbol{x} \leq \boldsymbol{x_{max}}, \\ & \boldsymbol{x} \in \mathbb{Z}, \\ & \boldsymbol{y_{min}} \leq \boldsymbol{y} \leq \boldsymbol{y_{max}}, \\ & \boldsymbol{g}(\boldsymbol{x},\boldsymbol{y}) \leq 0, \end{aligned} \tag{1}$$

where $\boldsymbol{x_{min}}$ and $\boldsymbol{y_{min}}$ are the lower boundaries, whereas $\boldsymbol{x_{max}}$ and $\boldsymbol{y_{max}}$ are the upper boundaries of the discrete and continuous design variables, respectively. Denoted as $\boldsymbol{g}$ above, all constraints in this study are implemented as inequality constraints.

Table 1: Design space of used design variables $\boldsymbol{x}$ and $\boldsymbol{y}$

Discrete $\boldsymbol{x}$		Continuous $\boldsymbol{y}$	
$\mathrm{P_{WT}}$	[5, 8, 10, 15] MW	$\mathrm{d_{easting}}$	[3:10] D
$\mathrm{U_{array}}$	[33, 66, 132] kV	$\mathrm{d_{northing}}$	[3:10] D
$\mathrm{U_{export}}$	[33, 66, 132, 220] kV	$\mathrm{s_{row}}$	[0:1] $\mathrm{d_{easting}}$
$\mathrm{n_{row}}$	[2:10] -	$\mathrm{s_{column}}$	[0:1] $\mathrm{d_{northing}}$
$\mathrm{n_{column}}$	[2:10] -	Ψ_{layout}	[-45:45] °
		$\mathrm{p_{lon.}}$	[-10:-9.2] °
		$\mathrm{p_{lat.}}$	[38.4:39.4] °

Table 1 shows the elements of the design parameter arrays $\boldsymbol{x}$ and $\boldsymbol{y}$ with their bounds divided into two categories, i.e. discrete and continuous variables. Discrete parameters include the integer values of decision variables such as turbine power $\mathrm{P_{WT}}$, inter-array cable voltage $\mathrm{U_{array}}$ and export cable voltage $\mathrm{U_{export}}$, which define the selection of turbine design and cable types. The latter two variables, $\mathrm{n_{row}}$ and $\mathrm{n_{column}}$, help to define the number of turbines in the wind farm. According to these inputs, first, turbines are placed in a regular rectangular layout. The

positioning of the turbines is realized with the help of a 5 degrees of freedom (DoF) layout model illustrated in Figure 1. The spacing between the rows and columns are respectively denoted by $d_{easting}$ and $d_{northing}$ in rotor diameters D of the selected turbine. The layout is free to rotate around the middle point by an angle Ψ_{layout}. Moreover, even numbered rows and columns are shifted by a distance defined by staggering ratio s_{row} and s_{column}, which are given as the fraction of respective spacings in both directions. These layout DoFs allow us to set the positions of each turbine in Easting-Northing plane, thus to generate a unique wind farm layout for a given set of design variables. It will ensure a structured shape of the layout and allow a decent degree of irregularity with column and row staggering. Unlike many wind farm optimization studies in literature obtaining irregular layouts, we opted for this parametrization so that the number of turbines (here $n_{row} \times n_{column}$) can be changed during the optimization, as opposed to formulating the problem on a fixed number of turbines. Finally, the last two continuous variables $p_{lon.}$ and $p_{lat.}$ represent the longitude and latitude coordinates of the site location.

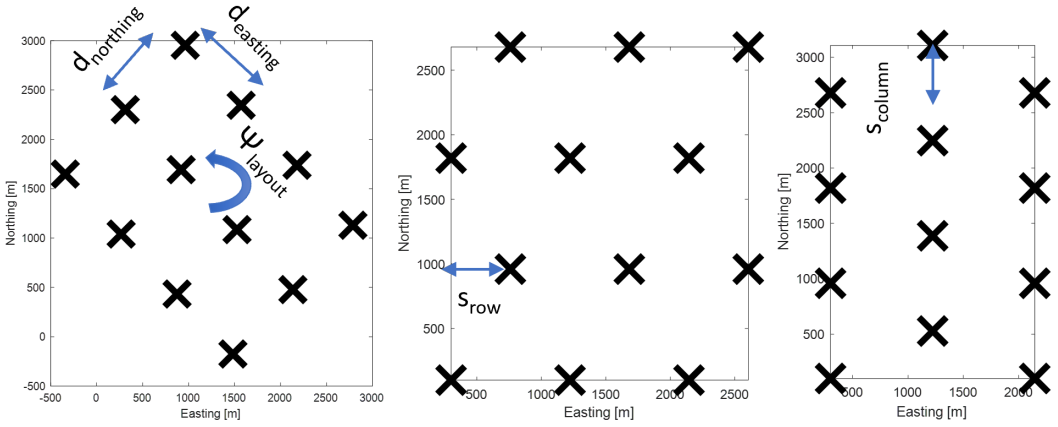

Figure 1: Illustration of wind farm layout DoFs starting from a rectangular layout

To calculate wind farm LCOE, the merit figure as a function of x in Equation 1, an in-house developed wind farm cost model requires a set of information regarding turbine and substructure design, farm layout, site characteristics, resource assessment, electrical infrastructure, installation and financial parameters. This wind farm model, called `CosMo-WF` (Cost Model for Wind Farms) [4], is developed in MATLAB in a modular structure with a work-flow depicted in Figure 2. The cost functions of different components and sub-systems are derived from raw data, reports, research and market studies available in the literature [5, 6, 7, 8]. LCOE, the ultimate metric used to assess the wind farm designs in this work, is calculated by the widely used definition:

$$LCOE = \frac{FCR \times CAPEX + OPEX}{AEP}, \tag{2}$$

where FCR stands for fixed charge rate, CAPEX are the capital expenditures and OPEX are operating expenses of a wind farm.

The detailed descriptions of the cost equations are out of scope of this paper. However, it is important to remark that each cable type characterized by the voltage value given in Table 1 has a different cost equation for unit length and a maximum capacity of rated power. This

maximum limit is used to find the number of turbines connected within an inter-array string. Correspondingly, it directly impacts the cable layout and resulting total length of inter-array cables. Likewise, the maximum power capacity of an export cable defines the number of export cables necessary for a given total wind farm power output and export cable voltage. Inter-array cable layout is modeled using a simplified algorithm to minimize cable lengths while avoiding cable crossings. A standard lazy wave configuration parameterized according to [9] is used to compute the length of the dynamic cables. For the sake of simplicity, only one substation is considered for all calculations, which is located at the centre of the farm.

Total wind farm AEP is calculated using the steady state engineering wake models in FLORIS [10], considering wind speed and wind direction probability distributions. By selecting P_{WT}, which represents the single unique turbine rating within the farm, the model inherits the look-up tables of power and thrust coefficients, which are retrieved from reference research turbines NREL 5MW [11], Leanwind 8MW [12], IEA 10MW [13] and IEA 15MW [14]. Based on these C_P and C_T curves, rotor diameter and hub height, FLORIS models the flow within the wind farm and calculates the power output of each turbine in a discrete manner at each wind speed and wind direction bin. A greedy wind farm control is implemented, meaning that all the rotor planes are always perpendicular to the incoming free-stream wind. Finally, total AEP is calculated by summing all the energy yields from every turbine and weighting them with the respective wind speed and direction probability on a given site. In the present work, the platform displacements and their impact on wake calculations are neglected.

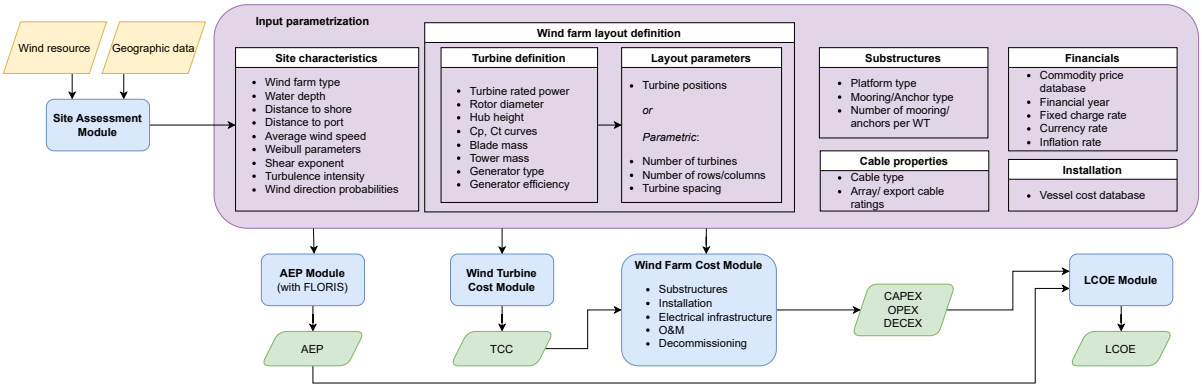

Figure 2: Wind farm cost model architecture

Due to the discontinuous nature of the problem and the presence of discrete variables, a mixed integer genetic algorithm is employed in Matlab. Each generation has a population of 300 design candidates and the function tolerance is set to 0.0001 €/MWh. In each generation, 30 designs (10% of *PopulationSize*) with best fitness function values are guaranteed to pass on to the next generation, using *EliteCount* option of Matlab's *ga* function. *CrossoverFraction* is set to 0.5 as a trade-off between efficient tracking of global optimum (high crossover rate) and better exploration of the whole design space (high mutation rate). This setting implies that 50% of the remainder 270 individuals (*PopulationSize* - *EliteCount*) are formed as a result of crossovers recombining design variables of individuals from previous generation, whereas the other 50% is formed by mutation allocating the design variables randomly.

2.2. Design constraints

The analysis includes the following design constraints:

- **Total power:** Maximum total power output allowed at the grid connection. It is set to 600 MW in present study.

- **Farm area:** The offshore area designated for wind farm development, A_{Farm}. Maximum value is taken 100 km^2 for present study.
- **Visibility:** The wind farm is to be located beyond a minimum distance from shore to minimize visual impact perceived by people on the shore. In order to quantify the visibility impact, visibility index (VI) formulation of Sullivan et al. [15] is employed, where VI is ranged from 1 (very low visibility) to 6 (strong visibility dominating the view). The empirical equation derived from daytime observations of various offshore wind farms relates the visibility to distance to shore d_{Shore} such that

$$VI = 7.3589\, e^{-0.037\, d_{Shore}}. \tag{3}$$

  In this work, VI of the wind farm is limited to 2 and 3 in two different optimization cases (named C2 and C3 in Section 3) to better understand the potential consequences of having visibility constraints on the wind farm design.
- **Availability:** No turbines should coincide with the exclusion zones designated by authorities. In this study, natural preserving areas are used as exclusion zones.
- **Water depth:** In order to focus on floating wind sites, current study investigates the sites where the water depth D_W is beyond 60m.
- **Water depth difference:** In this study, cost functions of a semi-submersible platform is used. To make a realistic case study, it is assumed that one single platform design is used for the entire wind farm. Therefore, it is necessary to ensure that the water depth difference within the farm ΔD_W is kept at an acceptable value in order to justify the applicability of a single platform design. Here, ΔD_W is constrained to a maximum of 100m, a reasonable range for a semi-submersible platform.
- **Mooring line distance:** Mooring lines are constrained to be at least 100m apart from each other ($d_{Mooring,min}$). In this work, the station-keeping of each semi-submersible floating platform is provided by three catenary mooring lines equally distributed by 120 degrees to each other. The first mooring line is always aligned with the main wave direction at a given site. To account for the mooring layouts, a simplified model for the mooring footprint radius $R_{Mooring}$ is adopted in a way that it is given as a function of water depth D_W using the catenary equation:

$$R_{Mooring} = \frac{T_H}{w} cosh^{-1}\left(\frac{D_W}{T_H/w} + 1\right) \times 1.1\ , \tag{4}$$

  where T_H is the horizontal design load at the fairlead attachment point and w is the mooring line equivalent unit weight in water. The constant term 1.1 on the right ensures that an additional 10% is added for the mooring line portion lying on the seabed. For the present study, a constant term for T_H/w is assumed for all turbine sizes. T_H is calculated by the rated thrust of NREL 5MW turbine (ca. 805 kN) multiplied with a safety factor of 2, whereas w is taken from the OC4 semi-submersible reference design (ca. 1065 N/m) [16].

2.3. Investigated area and site assessment

A case study on the Atlantic coast of Iberian Peninsula is performed. Figure 3 presents an overview of the inputs to the site assessment tool of the wind farm model. In Figure 3a, geographic information together with ports locations and exclusion zones are reported. Two types of areas, i.e. Natura 2000 and nationally designated nature reserves, are taken as exclusion

zones for wind farm site selection. The black frame in Figure 3a shows the focused area for the presented wind farm optimization study, which corresponds to the boundaries of $p_{lon.}$ and $p_{lat.}$ in Table 1.

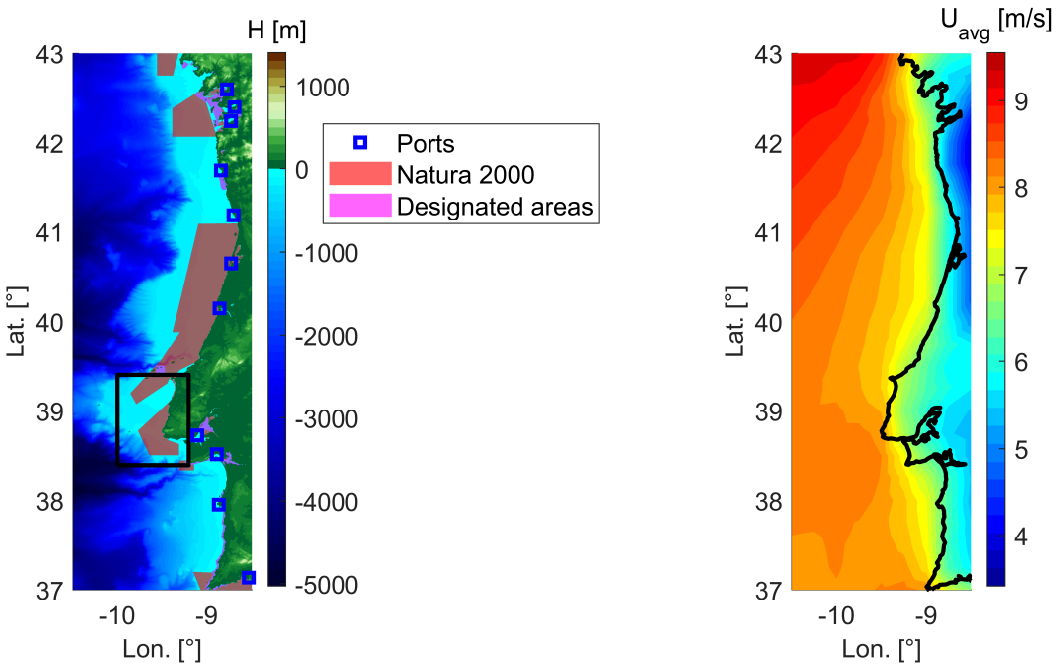

(a) Geographic input to wind farm model (b) Average wind speed input grid

Figure 3: Investigated area depicted on geographical data compiled from different sources [17, 18, 19]

Wind and wave resource of the given site is mapped using the hourly data of ERA5 reanalysis from the year 2022. As an example, the average wind speed grid at 100m height with the main shore line highlighted can be seen in Figure 3b. Using also the wind information at 10m height, a grid for vertical shear exponent is derived by the power law, which is then used to extrapolate the values from 100m to the corresponding hub heights of given wind turbine designs. At each grid point available in the dataset, hourly wind data is grouped into wind speed bins, which are then fitted into the Weibull probability function. This way, two separate input grids for Weibull shape and scale parameters are generated. On the other hand, wind direction is calculated taken into account the northerly and easterly components of the wind and binned into 30 degrees sectors. This practice allows us to build unique wind speed and direction distributions depending on the wind farm location as the optimizer moves from one position to another and interpolates the site characteristics accordingly. In addition to the wind information, main wave direction and significant wave height are imported into the wind farm model as well. As mentioned above, main wave direction is used to orientate the mooring lines, whereas the significant wave height is used for the OPEX calculation adapted from the work of Beiter et al. [6].

Open access data used in the study: As presented in this section, different data sets are used to define site characteristics, i.e. GEBCO Grid [17] for bathymetry and topography, EMODNET database [18] for exclusion zones and ports locations, and ERA5 data from Copernicus website [19] for wind and wave resource assessment.

3. Results

The design procedure is executed for two cases with different visibility constraints, i.e. $VI_{max} = 2$ and $VI_{max} = 3$, which are shortly presented here as C2 and C3. Required minimum distances from shore to wind farm site corresponding to these VI values are ca. 35.2km and 24.3km, respectively. Results of the optimal design arrays are reported in Table 2.

First 3 discrete variables $\mathrm{P_{WT}}$, $\mathrm{U_{array}}$ and $\mathrm{U_{export}}$ have converged to same values. It is as expected to see that the optimizer chooses the biggest turbine available. Given the fact that the wind farm area is constrained, and this constraint is well utilized (see A_{Farm} in Table 3), in other words it is an active constraint defining the design, the biggest turbine would provide the most energy yield with minimum wake losses due to more sparsely populated wind farm layout. Inter-array cable of 33kV is found to be the trade-off between unit price of dynamic cables and cable lengths. The resulting combination of $\mathrm{U_{array}}$ and $\mathrm{P_{WT}}$ leads to only 2 turbines per string complying with the maximum power capacity of the cable. Although this amplifies the cable distances required to be covered due to the fact that for every new string the distance from the first turbine to the substation is added, the additional unit price of higher voltage cables compared to 33kV does not compensate this increase in total cable length. Here, the position of the substation might play an important role too. In this work, a single offshore substation is implemented and is always positioned at the middle of the layout. In fact, this tends to decrease the inter-array cable lengths and therefore the optimizer favors the low voltage cable type. Different positioning of the substations depending on project specific conditions might yield different results. In both cases, the optimal number of turbines is found to be 40 ($\mathrm{n_{row}} \times \mathrm{n_{col.}}$), which leads to the total rated wind farm power of 600MW, the maximum value prescribed by the constraint definition. Since both designs converged to 220kV export cable, again following the maximum cable capacity, two cables are required to transmit the electricity from offshore substation to the land.

Case	$\mathrm{P_{WT}}$	$\mathrm{U_{array}}$	$\mathrm{U_{export}}$	$\mathrm{n_{row}}$	$\mathrm{n_{col.}}$	$\mathrm{d_{easting}}$	$\mathrm{d_{northing}}$	$\mathrm{s_{row}}$	$\mathrm{s_{col.}}$	Ψ_{layout}
C2	15MW	33kV	220kV	10	4	8.51D	4.90D	0.34	0.95	13.4°
C3	15MW	33kV	220kV	5	8	6.09D	6.98D	0.01	0.47	-15.9°

Table 2: Optimized solutions $[\boldsymbol{x}, \boldsymbol{y}]$ for different constraints

Having looked at the discrete decision variables, the optimal layouts and site locations as a result of continuous variables in Table 2 can be analyzed. We found the optimal site coordinates $[\mathrm{p_{lon.}}, \mathrm{p_{lat.}}]$, i.e. midpoint of the farm layout, at [-9.888593°, 38.867967°] for C2 and [-9.816336°, 38.801265°] for C3 layout. In Figure 4, the boundaries of the two optimal layouts, which are calculated as the convex hull of all turbine and anchor positions on Easting-Northing plane, are depicted. It is clearly seen that C3 layout is positioned at the edge of the exclusion zones, meaning that the design driver for this wind farm siting is the environmental constraint. On the other hand, C2 wind farm position is mainly driven by the visual impact constraint, as its d_{Shore} (see Table 3) corresponds to the maximum VI allowed, which is 2.

Case	A_{Farm}	$D_{W,avg}$	ΔD_W	d_{Shore}	d_{Port}	$d_{Mooring,min}$
C2	94.7 $\mathrm{km^2}$	118.1 m	35.8 m	35.2 km	75.2 km	449 m
C3	93.5 $\mathrm{km^2}$	92.5 m	80.8 m	27.7 km	66.8 km	716 m

Table 3: Constraints comparison between optimal solutions from C2 and C3

In Figure 5, the optimized layouts are displayed more in detail. Since two optimized wind

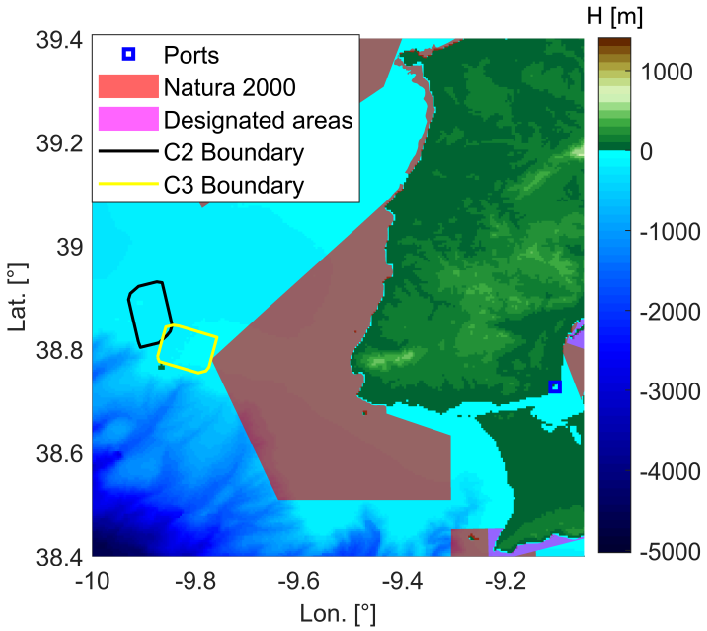

Figure 4: Optimized wind farm designs with varying distance to shore constraints

farm locations are close to each other, their met-ocean characteristics are similar. This is directly observed from the similar mooring line orientations, since both sites show a main wave direction of ca. 309° North-West. Similarly, the most probable wind directions are 360° North and 330° North-West for both sites, for which the optimizer found the most suitable combination of layout DoFs to minimize wake losses. Although it could have been beneficial to have narrow and long rectangular layouts facing the main wind direction from power maximization point of view, more square layouts are favoured to keep turbines close to the centre, namely the substation, to minimize cable lengths.

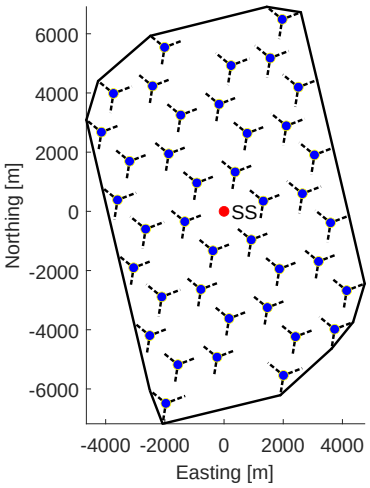

(a) C2 Layout

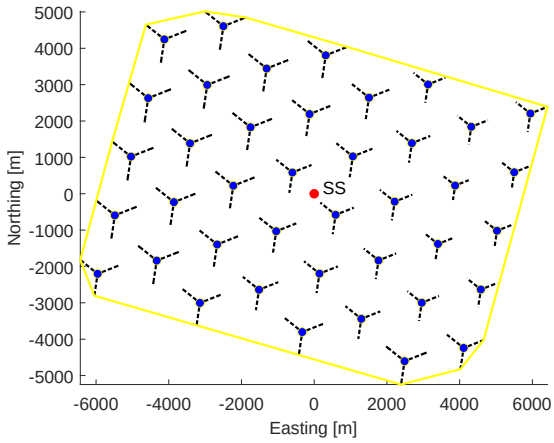

(b) C3 Layout

Figure 5: Optimal wind farm layouts. Blue dots represent turbine positions. Red dot shows substation (SS) position. Dashed lines are projected mooring line lengths seen from above.

As observed by the comparison of two optimal layouts, C3 displays more variability in mooring line lengths, attributed to the steeper seabed slope compared to C2. In fact, ΔD_W of C3 is closer to the upper limit of 100m (see Table 3). It can be interpreted that this constraint played a significant role on the optimal layout orientation, more in particular the layout rotation DoF Ψ_{layout}. Nevertheless, both layouts appear to be optimized mainly for AEP maximization, since the minimum mooring line distance constraints $d_{Mooring,min}$ are well satisfied for both cases.

	AEP	CAPEX	OPEX	LCOE
C2/C3 - 1	-0.55%	+2.35%	+1.30%	+2.46%

Table 4: Relative comparison of cost of energy between optimal solutions from C2 and C3

Relative comparison of key indicators from both wind farm designs are reported in Table 4. This table can be interpreted as the cost of moving from $VI_{max} = 3$ to $VI_{max} = 2$ in this case study. The decrease in AEP, hence the decrease in capacity factor, is directly related to differences in layout and wind conditions. Although in this case the change in wind resource is minor, a slight increase of Weibull probabilities for above-rated wind speeds at C3 site is enough to create this difference. CAPEX and OPEX increase depends on mainly higher D_W, d_{Shore} and d_{Port}, which are all significant inputs to the installation, electrical infrastructure and O&M modules in the wind farm cost model. Finally, as a result of the discussed effects, LCOE is increased by 2.46%, which suggests a non-negligible economical impact of visibility constraints.

4. Conclusions

A novel wind farm design methodology is proposed, integrating several design variables from different design aspects into an optimization problem. The objective function of the optimization problem is formulated as LCOE, which is estimated by a comprehensive wind farm cost model. To demonstrate the sensitivity of the design constraints, a floating wind farm on the Atlantic coast of the Iberian Peninsula is sited and optimized as a case study. The results showed a 2.46% difference in terms of LCOE between two optimal wind farm designs with two different visibility constraints, which implicitly impose a minimum limit on the distance to shore from the wind farm. In addition to the common wind farm design constraints such as total electrical power at the grid connection and total wind farm area, exclusion zones are incorporated in the design problem to allow the site selection only in the areas suitable for wind farm development. These results reveal the importance of wind farm design constraints and highlights the complexity of the wind farm design optimization, where many design parameters are interacting with each other and an integrated design approach is required to reduce the number of design iterations during the early planning phase. The developed tool in this work might have a potential to bridge the gap between wind farm developers and local authorities who are responsible for permitting and zoning of development areas, which might help to reduce the permitting times and the costs involved during these processes. Future work is to extend this analysis to further case studies on different sites and incorporating floating effects on wind farm calculations due to platform movements for more accurate AEP estimations.

Acknowledgement

This work has been conducted within the FLOAWER project. This project has received funding from the European Union's Horizon H2020 research and innovation programme under the Marie Skłodowska-Curie grant agreement N°860579.

References

[1] Díaz H, Silva D, Bernardo C and Soares C G 2023 *Renewable Energy* **204** 449–474
[2] Sanchez Perez Moreno S 2019 *A guideline for selecting MDAO workflows with an application in offshore wind energy* Ph.D. thesis Delft University of Technology
[3] Hietanen A I, Snedker T H, Dykes K and Bayati I 2023 *Wind Energy Science Discussions* **2023** 1–31
[4] Yilmazlar K, Cacciola S, Rodriguez M X A and Croce A 2022 *Journal of Physics: Conference Series* vol 2265 (IOP Publishing) p 042042
[5] Fingersh L, Hand M and Laxson A 2006 Wind turbine design cost and scaling model Tech. rep. National Renewable Energy Lab.(NREL), Golden, CO (United States)
[6] Beiter P, Musial W, Smith A, Kilcher L, Damiani R, Maness M, Sirnivas S, Stehly T, Gevorgian V, Mooney M *et al.* 2016 A spatial-economic cost-reduction pathway analysis for us offshore wind energy development from 2015–2030 Tech. rep. National Renewable Energy Lab.(NREL), Golden, CO (United States)
[7] Rosenauer E 2014 Investment costs of offshore wind turbines Tech. rep. University of Michigan Center for Sustainable Systems, Ann Arbor, MI (United States)
[8] Topper M B, Nava V, Collin A J, Bould D, Ferri F, Olson S S, Dallman A R, Roberts J D, Ruiz-Minguela P and Jeffrey H F 2019 *Renewable and Sustainable Energy Reviews* **112** 263–279
[9] Rentschler M U, Adam F and Chainho P 2019 *Renewable and Sustainable Energy Reviews* **111** 622–635
[10] NREL 2021 Floris. version 2.4 URL `https://github.com/NREL/floris`
[11] Jonkman J, Butterfield S, Musial W and Scott G 2009 Definition of a 5-mw reference wind turbine for offshore system development Tech. rep. National Renewable Energy Lab.(NREL), Golden, CO (United States)
[12] Desmond C, Murphy J, Blonk L and Haans W 2016 Description of an 8 mw reference wind turbine *Journal of Physics: Conference Series* vol 753 (IOP Publishing) p 092013
[13] Bortolotti P, Tarres H C, Dykes K L, Merz K, Sethuraman L, Verelst D and Zahle F 2019 Iea wind tcp task 37: Systems engineering in wind energy-wp2. 1 reference wind turbines Tech. rep. National Renewable Energy Lab.(NREL), Golden, CO (United States)
[14] Gaertner E, Rinker J, Sethuraman L, Zahle F, Anderson B, Barter G E, Abbas N J, Meng F, Bortolotti P, Skrzypinski W *et al.* 2020 Iea wind tcp task 37: definition of the iea 15-megawatt offshore reference wind turbine Tech. rep. National Renewable Energy Lab.(NREL), Golden, CO (United States)
[15] Sullivan R G, Kirchler L B, Cothren J and Winters S L 2013 *Environmental Practice* **15** 33–49
[16] Robertson A, Jonkman J, Masciola M, Song H, Goupee A, Coulling A and Luan C 2014 Definition of the semisubmersible floating system for phase ii of oc4 Tech. rep. National Renewable Energy Lab.(NREL), Golden, CO (United States)
[17] GEBCO Compilation Group (2023) `https://www.gebco.net/`
[18] European Marine Observation and Data Network (EMODnet) `https://emodnet.ec.europa.eu/`
[19] Copernicus Climate Data Store - ERA5 hourly data on single levels from 1940 to present `https://cds.climate.copernicus.eu/`